Spatial Correlation of PAN UWB-MIMO Channel Including User Dynamics

Wang, Yu; Kovacs, Istvan Zsolt; Pedersen, Gert Frølund; Olesen, Kim

Publication date:
2007

Document Version
Publisher's PDF, also known as Version of record

EUROPEAN COOPERATION
IN THE FIELD OF SCIENTIFIC
AND TECHNICAL RESEARCH

EURO-COST

COST 2100 TD(07) .....
Duisburg, Germany
2007/ Sept /10-12

SOURCE: Department of Electronic Systems,
Aalborg University,
Denmark

Spatial Correlation of PAN UWB-MIMO Channel Including User Dynamics

Yu Wang, István Z. Kovács, Gert F. Pedersen and Kim Olesen
Deparment of Electronic Systems
Niels Jernes Vej 12
9220 Aalborg
Denmark
Phone: + 45-9635 8630
Fax: + 45-9815 1583
Email: yw@es.aau.dk, istvan.kovacs@nsn.com, gfp@@es.aau.dk, ko@es.aau.dk

Spatial Correlation of PAN UWB-MIMO Channel Including User Dynamics

Yu Wang, István Z. Kovács, Gert F. Pedersen and Kim Olesen

***Abstract*—In this paper we present and analyze spatial correlation properties of indoor 4x2 MIMO UWB channels in personal area network (PAN) scenarios. The presented results are based on measurement of radio links between an access point like device and a hand held or belt mounted device with dynamic user. It is found the channel shows spatial correlated wideband power, and spatial uncorrelated complex channel coefficients at different frequencies and delays with respect to a correlation coefficient threshold of 0.7. The Kronecker model is proved not suitable for the investigated scenarios. The MIMO UWB channel achieves an ergodic capacity close to i.i.d. Rayleigh channel capacity. However the outage capacity degrades due to the wideband power fluctuation / shadowing introduced by user's body.**

***Keywords*—Ultra wideband, spatial correlation, multi-input multi-output, personal area network, user dynamics, capacity**

I. Introduction

The Ultra wide band (UWB) technology has been one of the most popular topics among the communications research community since the 1990's due to its potential on the high data rate and/or reliable transmission with low transmission power. The frequency selective nature of UWB channels makes the fading of wideband power much smaller than other communication systems. However, the rigid power constrains, regulated by regulator bodies e.g. FCC and ETSI, make the design of a UWB system a big challenge.

The combination of UWB and multi-input multi-output (MIMO) techniques is considered as a potential solution, to improve reliability and coverage, increase the data rate and reduce power consumption of UWB systems. Being aware of the strong limitations imposed on UWB communications by regulation bodies, the UWB-MIMO system was justified from different aspects including additional capacity enhancement [1] [2] and extra diversity and coding gains [3] [4] [5]. The performance of such systems was shown dependent upon 1 spatial correlation properties between transmission links. The spatial correlation of UWB multiple antenna systems based on indoor channel measurements was investigated in [1], [6], [7] and [8]. Tthe spatial correlation was characterized either in the frequency domain [1], [6], [7] or the delay domain [8].

The UWB technology is considered as a candidate PHY solution for body-centric personal area network (PAN) communications which is characterized by short range and low power wireless links. In PAN environments a significant impact of the user proximity and user dynamics on the signal propagation was disclosed since transceivers are often body worn or hand held devices [9]. The spatial correlation properties of MIMO radio channels in such PAN scenarios are also expected to be time variant because of the user movements [9] [10].

In this paper, the spatial correlation of multi-antenna UWB channels was investigated in PAN scenarios based on experimental data in the lower UWB frequency band of 3-5 GHz with 4 receive antennas and 2 transmit antennas [9] [10]. Compared with previous studies our measurement was unique in the antenna configurations and the scenarios with dynamic users.

The spatial structure of the channel was unveiled and a Kronecker model was evaluated in the view of UWB MIMO channel modeling. The capacity of the measured UWB-MIMO channel was evaluated.

The paper is organized as follows. Section II describes the experimental work and the scenarios. Section III presents the data analysis and processing. In Section IV the MIMO spatial correlation analysis is presented. Finally, the paper is ended by a conclusion in Section V.

II. Measurement Setup and Environment

The radio channel measurements were conducted with a time domain UWB sliding correlator channel sounder. The measurement bandwidth was 2.5 GHz centered at 4.5 GHz. The effective delay resolution was 0.4 ns [10].

A linear array of four UWB planar monopoles was used at the access point (AP) (Fig.1 right), and two cylindrical monopoles were used in user devices (UD) (Fig.1 left). The antenna separation distance was $\lambda/2$ at both AP and UD, where λ=6.7cm is the wavelength at center frequency 4.5 GHz. A more detailed description of the measurement system can be found in [10].

Table I summarizes the main characteristics of the measurement environments and radio channels. In all scenarios the UD was carried by users at 1 m height from the room's floor and with $v\approx$1m/s speed. Three typical environments, laboratory (LAB), conference room (CAN) and hallway (HAA) have been investigated with user routes, covering the most likely user movement patterns relative to the location of the AP. As an example, the layout of the conference room environment is shown in Fig.2.

The main difference between the three environments is in the AP height, which leads to a different signal clustering in the channel impulse response (CIR). Furthermore, in the LAB environment the density of the scattering objects (furniture, equipment, etc.) was much higher compared to the CAN and HAA environments.

Table I

Main Characteristics of the measurement environments and user routes [10]

Environment	Area Dimension WxLxH (m)	AP height (m)	AP-UD range (m)	Rms delay spread (ns)	Number of routes
LAB	8x14x2.3	2.3	2-7	13	3
CAN	15x17x2.3	2.3	2-7	25	5
HAA	12x17x11	6	6-17	35	6

The number of routes measured in each environment is listed in Table I. Approximately a number of 25 different measurements runs were taken in each scenario with different users and moving directions. The radio channel sampling rate was 40Hz, i.e. every 0.025 s a MIMO snapshot containing 4x2=8 simultaneously measured radio links was recorded. The duration of each measurement route was either 12.5 s or 25 s depending on the length of the route. Therefore, in total more than 10,000 MIMO channel snapshots were measured.

Unless otherwise stated, the statistical results shown in the following sections were based on measured data from all the environments

III. Data Analysis and Processing

A. *Stationarity of the measured channel*

The wideband power is considered as stationary over the whole measurement route since the path loss effect is almost negligible compared with body shadowing for the measured scenarios.

The complex channel coefficients at different frequencies and delays are non-stationary due to the dynamics of the user. The non-stationarity was caused by the variation of the scatterers when user moved in the environment. The channel may be treated as stationary over a short interval. To identify the channel stationarity a quantified metric was applied to the measured channels in order to obtain stationary interval.

The metric is similar to the one proposed in [11]. First, the averaged power delay profile over all links was computed by,

$$PDP(t,\tau)=\frac{1}{L}\sum_{l=1}^{L}\left|h(t,\tau,l)\right|^2 \quad (1)$$

where $h(t,\tau,l)$ is the complex channel coefficient at time t, delay τ and SISO link l and L is the total number of SISO links. Then the small scale fading was averaged out by performing sliding window time averaging with a window length of 10 channel samples which produces $\overline{\mathrm{PDP}(t',\tau)}$. The time-domain PDP correlation metric used is defined as:

$$\rho_{\overline{PDP}}(\Delta t')=\frac{\sum_\tau \overline{PDP}(t_0',\tau)\cdot\overline{PDP}(t_0'+\Delta t',\tau)}{\max\left\{\sum_\tau(\overline{PDP}(t_0',\tau))^2,\sum_\tau(\overline{PDP}(t_0'+\Delta t',\tau))^2\right\}} \quad (2)$$

and decreases when channel wideband power and/or structure of $\overline{\mathrm{PDP}}$ varies significantly between the two time instances $\Delta t'$ apart. Therefore $\rho_{\overline{\mathrm{PDP}}}(\Delta t')$ is used as an indicator of channel stationarity, i.e. the interval during which $\rho_{\overline{\mathrm{PDP}}}(\Delta t')$ is greater than a predefined threshold $C_{th}=0.5$ is considered as stationary as recommended in [11].

Fig.1 Antenna setup for the measurement setup, left: handheld user device (UD); right: access point device (AP)

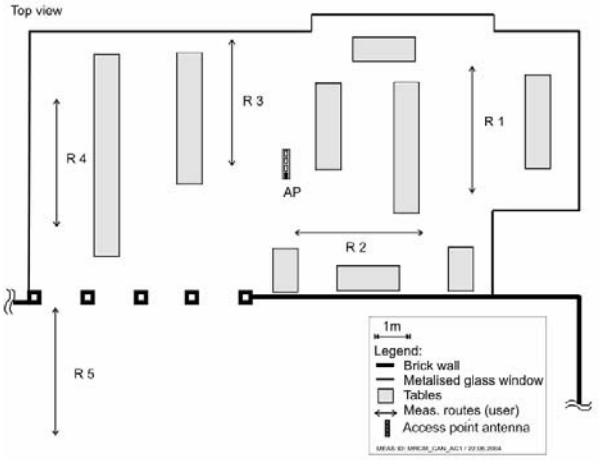

Fig.2 Layout of Conference Room (CAN) environment

Only blocks with more than 50 samples were used in this paper. And statistical results based on a large amount of measurement data were obtained to ensure the reliability of the analysis.

B. *Spatial correlation*

The measured time-varying UWB-MIMO channels can be expressed either in time-delay domain as **H(t, τ)**, or in time-frequency domain as **G(t, f)**. In this study the channels was investigated in both time-frequency and time-delay domains.

The presence of orthogonal MIMO links is a necessary condition to realize the linear increase in MIMO capacity [12]. The spatial correlation between the links is an important measure to identify the independence of the links.

The correlation coefficient was calculated between each pair of the links. It is expressed as

$$\rho_{(m1n1,m2n2)}=<\beta_{m1n1},\beta_{m2n2}> \quad (3)$$

where <...> is the correlation coefficient operation, and defined as

$$<a,b>=\frac{E[ab^*]-E[a]E[b^*]}{\sqrt{(E[|a|^2]-|E[a]|^2)(E[|b|^2]-|E[b]|^2)}} \quad (4)$$

where .* is the complex conjugate ad E[.] denotes expectation.

By replacing β with h(t,τ), g(t,f) and p(t) in Eq (3), the spatial correlation in the delay domain ρ_{delay}, frequency domain ρ_{freq} and wideband power ρ_{pow} is obtained respectively, where h(t,τ) and g(t,f) are elements in **H(t, τ)** and **G(t, f)**, and

$$p(t) = \sum_{\tau} |h(t,\tau)|^2 \quad (5)$$

ρ_{delay} and ρ_{freq} are calculated within each stationary time block defined based on Eq (2), and ρ_{pow} is calculated over the whole measurement route.

In this work we use a threshold of 0.7 for the correlation coefficient to be considered as 'correlated'.

IV. Analysis Results

A. Spatial correlation of wideband power (ρ_{pow})

Due to the large bandwidth of the investigated channel, there is no fading in the wideband power. The spatial correlation of the wideband power is mainly introduced by body shadowing. Therefore the wideband power at the receiver is correlated since the receiver antennas usually see the same shadowing. On the contrary the transmitter which is belt-mounted or hand-held by the users can undertake different shadowing, hence lower spatial correlation.

This is proved by Fig.3 (left) which plots the mean spatial correlation of wideband power. The upper left and lower right corners of the figure correspond to the spatial correlation at the receiver refer to the two transmitter antennas respectively. They are significantly higher than the correlation between other links as expected.

B. Spatial correlation of complex channel coefficients at different delays (ρ_{delay})

The mean and 10% CDF spatial correlation at different delays is illustrated in Fig.4. The 10% CDF refers to the value which is higher than 90% of data. The mean spatial correlation is approximately 0.5 in the first delay bin, and decays to about 0.3 in 20 ns. Similar results were reported in [8]. The 10% CDF correlation is only significant, i.e. above 0.7, for the first 5 ns delay spread, in general corresponding to the most significant direct signal paths. A correlation of 0.6 was observed between spatial correlation and channel gains at different delays. It implies a smaller angular spread for the clusters containing more power, e.g. the direct or main reflection clusters.

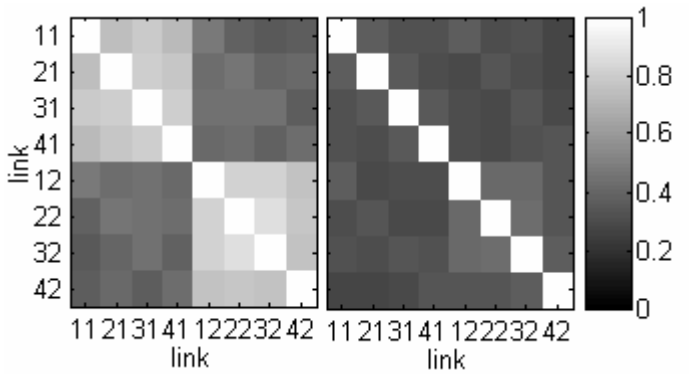

Fig.3 Mean spatial correlation of different link-pairs

Left: ρ_{pow}; right: ρ_{freq}. Link "41" indicates the link between receive antenna #4 and transmit antenna #1.

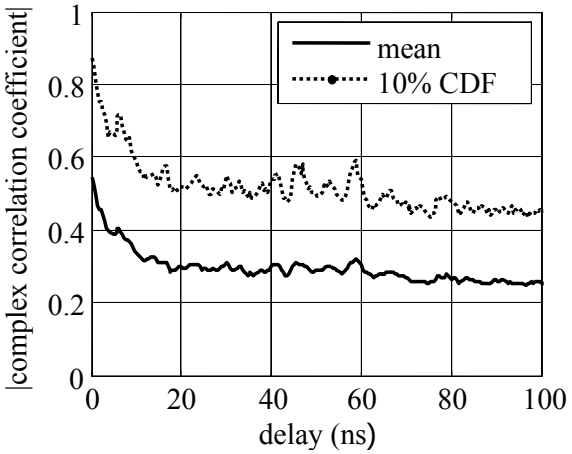

Fig.4 Mean and 10% CDF spatial correlation at different delays

C. Spatial correlation of complex channel coefficients at different frequency (ρ_{freq})

The spatial correlation does not show differences in the mean and 10% CDF values at different frequencies within the whole frequency band. Both mean (Fig.3 right) and 10% CDF correlation are below 0.6, which implies the potential of spatial diversity.

To identify the variation of the spatial correlation respect to frequency separations, a metric called correlation matrix distance (CMD) was used. The CMD was originally proposed in [13] to describe the non-stationarity of MIMO channels. Here we define the modified CMD as

$$CMD(f_1, f_2) = 1 - \frac{|tr\{R(f_1)R(f_2)\}|}{\|R(f_1)\|_F \|R(f_2)\|_F} \quad (6)$$

where $\|\bullet\|_F$ represents Frobenius norm.

The CMD becomes zero for identical correlation matrices and unity for maximally differed matrices. When the CMD is greater than 0.2 [13], the channel matrix undertakes a significant change. Fig.5 shows the CMD varies faster, and reaches 0.2 with a 5, 40 and 100 MHz frequency separation in the HAA, LAB and CAN environment respectively.

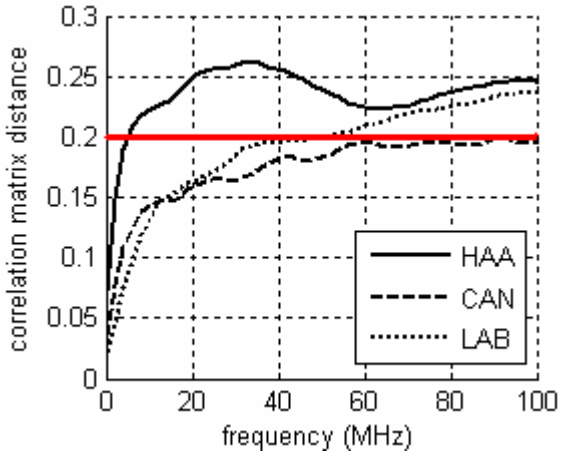

Fig.5 Mean correlation matrix distance with respect to frequency separations in different environments

D. Spatial correlation at transmitter and receiver

The receiver and transmitter correlation measures analyzed here represent spatial correlations between two radio links sharing the same transmit and receive antenna respectively. The correlation between other link pairs is referred as 'others'.

The difference of ρ_{pow} at the transmitter and receiver sides has been discussed in Section IV-A. For the ρ_{delay} and ρ_{freq}, the transmitter and receiver correlations are normally different due to antenna configurations, richness of local scatterers, user movements, etc. Table II shows mean and 10% CDF spatial correlation at transmitter and receiver.

In our measurement system, the antenna elements separation was the same at transmitter and the receiver with 0.5λ. The receiver antenna array was always fixed on the ceiling, therefore it yield a higher spatial correlation. However, the difference is not significant, and both at the transmitter and the receiver the channel is spatially uncorrelated due to the rich scatters in all the investigated environments. Furthermore, at the transmitter side the antenna near field effects due to the user proximity may result in different radiation patterns for transmitter antenna elements which decrease the correlation.

E. Spatial correlation with different Rx antenna spacing

The receive correlation is further analyzed in terms of antenna elements separation in this section. Table III shows the mean and 10% CDF receiver spatial correlation with different antenna spacing. The results show that the antenna spacing ranging from λ/2 to 3λ/2 has little effect on the ρ_{delay} and ρ_{freq}. And they are always uncorrelated with all antenna separations.

The effects of the antenna separation are more considerable for the ρ_{pow}. However, the channel is always spatially correlated for the wideband power. Therefore, from a system perspective the deployment of a selection diversity scheme at the access point like device based on wideband power measurements requires an antenna elements spacing of at least 3λ/2.

Table II

Mean and 10% CDF spatial correlation at receiver (Rx) and transmitter (Tx)

	ρ_{delay}		ρ_{freq}		ρ_{pow}	
	mean	10%	mean	10%	mean	10%
Rx	0.35	0.63	0.38	0.65	0.84	0.95
Tx	0.30	0.53	0.34	0.60	0.57	0.84
Others	0.27	0.49	0.30	0.56	0.51	0.80

Table III

Mean and 10% CDF receiver spatial correlation with different antenna spacing

	ρ_{delay}		ρ_{freq}		ρ_{pow}	
	mean	10%	mean	10%	mean	10%
0.5 λ	0.35	0.63	0.38	0.65	0.83	0.95
λ	0.32	0.58	0.34	0.60	0.80	0.93
1.5 λ	0.31	0.55	0.33	0.58	0.75	0.93

F. Spatial structure of the measured channel

In PAN environments the transmitter and receiver are usually located in the same cluster of scatterers due to the short range of transmission. Therefore we expect that the spatial correlation at the receiver side is not completely independent from the spatial correlation at the transmitter side. This is contrary to one assumption of a well known Kronecker model for MIMO channels, which was proved to be valid for both outdoor [14] and indoor [15] MIMO channel modeling with certain antenna configurations. In the Kronecker model the channel covariance matrix is estimated as

$$\rho_{(m1n1,m2n2)}^{[Kron]} = \overline{\rho}_{(Rx,m1m2)}^{[Kron]} \bullet \overline{\rho}_{(Tx,n1n2)}^{[Kron]} \tag{7}$$

where

$$\overline{\rho}_{(Rx,m1m2)}^{[Kron]} = E\left[< \beta_{m1n}, \beta_{m2n} > \right], n \in [1,2] \tag{8}$$

$$\overline{\rho}_{(Tx,n1n2)}^{[Kron]} = E\left[< \beta_{mn1}, \beta_{mn2} > \right], m \in [1,2,3,4] \tag{9}$$

And the model error is defined as:

$$\Psi = \frac{\left\| R - R_{Kron} \right\|_F}{\left\| R \right\|_F} \tag{10}$$

where R and R_{Kron} are channel correlation matrix whose elements are $\rho_{(m1n1,m2n2)}$ and $\rho_{(m1n1,m2n2)}^{[Kron]}$ respectively.

For the ρ_{delay} and ρ_{freq}, the model error is unreliable since they are calculated with limited number of samples. From Table II it is clear that the mean correlation of link pairs without common antennas is much larger than the product of the mean receiver and transmitter correlation, which violates the Kronecker model assumption specified in Eq(7). It is shown in the previous sections that for the ρ_{delay} and ρ_{freq}, all link-pairs exhibited similar cross correlation. With respect to an ideal spatially white case whose channel matrix is an i.i.d. random matrix [16], the investigated channel is called quasi spatially white. It is characterized by non-zero correlation due to the insufficient richness of the scattering to provide fully decorrelate links and small difference in the correlation of different link pairs.

For the ρ_{pow} as explained in the Section IV-A the correlation is caused by body shadowing instead of local scatterers. Interestingly, the Kronecker model shows fitness for some of the measurement routes. It's because the effects of body shadowing at the transmitter and receiver can be separated. Table IV summarizes the model error of ρ_{pow} in the different environments with 4-by-2 or 2-by-2 antenna configuration. . Since the number of samples (520) to calculate the ρ_{pow} is still not sufficient to achieve accurate correlation, a model error less than 4% is considered as a good fit. For the 2-by-2 antenna configuration, overall the Kronecker model is suitable for 1/4 of the measurement routes.

Table IV

Model error of ρ_{pow}	LAB		CAN		HAA	
	4x2	2x2	4x2	2x2	4x2	2x2
Mean	9.8%	6.9%	16.9%	10.2%	13.3%	6.1%
Std	3.9%	4.7%	9.2%	6.0%	10.2%	3.5%
% of routes with error<4%	0	25	0	12.5	8.3	33.3

G. *Capacity*

To calculate channel capacity, the UWB-MIMO channel first normalized to ensure that

$$E_{t,f}\left[\left\|G_{norm}(t,f)\right\|_F^2\right] = N_{Tx}N_{Rx} \quad (11)$$

This normalization retains the relative power fluctuations for each measurement route.

With the assumption of no channel state information (CSI) at the transmitter and perfect CSI at the receiver, the sub-band and wideband capacity in [bit/s/Hz] are defined as,

$$C_{SB}(t,f) = \log_2\left[\det(I_{N_{Rx}} + \frac{SNR}{N_{Tx}} G_{norm}(t,f) G_{norm}(t,f)^*)\right] \quad (12)$$

$$C_{WB}(t) = \frac{1}{B}\int_B C_{SB}(t,f)df \quad (13)$$

where SNR is a receiver signal to noise ratio which is selected to be 10 dB, I is an identity matrix, (*) means transpose-conjugate, $\det(\bullet)$ denotes the determinant and B is the bandwidth of measured channel which is 1 GHz in our study.

The ergodic and 1% outage capacity at 10 dB SNR is shown in Fig.6. The increase of the MIMO ergodic capacity respect to the SISO channel and of the wideband outage capacity respect to the narrowband channel are both significant. The ergodic and 1% outage capacity for the MIMO UWB channel is 5.4 b/s/Hz and 4 b/s/Hz respectively. Compared to the i.i.d. Rayleigh channel capacity, the outage capacity drops approximately 25% mainly due to the signal shadowing introduced by users' body and movements.

The capacity with three different antenna configurations, 4x2 MIMO, 2x2 MIMO and 2x2 MIMO with 2 extra antennas on the receiver providing selection diversity, was evaluated. It is shown in Fig.7 that by increasing the MIMO from 2x2 to 4x2 the ergodic capacity increases about 12% and adding two extra antennas on the receiver side providing selection diversity can improve the outage capacity by about 10%.

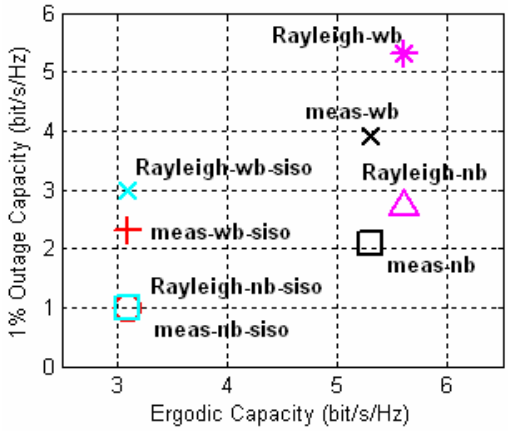

Fig.6 Ergodic and 1% outage capacity of the measured channels

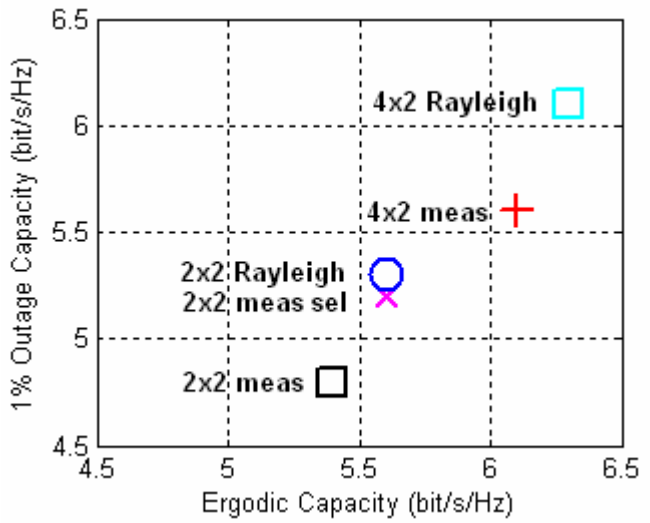

Fig.7 Ergodic and 1% outage capacity of the measured channels with different antenna configurations

V. Conclusion

In this paper we presented an analysis of the spatial correlation properties of indoor PAN UWB-MIMO channels based on the channel measurement of radio links between an access point like device and a dynamic user with hand held or belt mounted device It is found the channel shows spatial correlated wideband power, and spatial uncorrelated complex channel coefficients at different frequencies and delays with respect to a correlation coefficient threshold of 0.7. In both time-frequency and time-delay domain, the investigated PAN UWB-MIMO channel was found to be quasi spatially white since all link pairs showed similar correlation properties. The Kronecker model was proved not suitable for these PAN scenarios where the receiver and transmitter are located in the same cluster of main radio scatterers. A quarter of the measurement routes show fitness of the Kronecker model in the spatial correlation in the wideband power. It is because the effects of body shadowing, which introduces the correlation, can be separated at the transmitter and the receiver sides. Since the body shadowing usually is the same at all receiver antennas and different at transmitter antennas, the wideband power is spatially correlated at the receiver and uncorrelated at the transmitter. In the time-delay domain only the 10% CDF correlation of the first 5 ns is higher than 0.7 and the spatial correlation was found to be correlated with the channel gain at different delays. In the time-frequency domain the spatial correlation was disclosed to be independent over frequency offsets ranging from 2 MHz to 30 MHz depending on the radio environment. This information is useful for frequency domain UWB MIMO channel modeling in similar PAN scenarios and further for the optimization of the frequency-domain link-adaptation and packet scheduling algorithms. The ergodic and 1% outage capacity of the measured channel were determined to be 5.4 b/s/Hz and 4 b/s/Hz at 10 dB SNR. And the 1% outage capacity drops approximately 25% mainly due to the signal shadowing introduced by users' body and movements.

ACKNOWLEDGMENT

This paper describes work partially undertaken in the context of the IST-FP6/2002/IST/1, ”My personal Adaptive Global Net” (IST-2004-507102 MAGNET, www.ist-magnet.org), in WP3.1”PAN Radio Channel Measurements and Models”.

00Reference

[1] W. Q. Malik, M. C. Mtumbuka, D. J. Edwards, and C. J. Stevens, "Performance analysis of ultra-wideband spatial MIMO communications systems," in *IST Mobile Comm.Summit.* 2005.

[2] F. Zheng and T. Kaiser, "On the Evaluation of Channel Capacity of Multi-Antenna UWB Indoor Wireless Systems," in *International Symposium on Spread Spectrum Techniques and Applications, ISSSTA* 2004, pp. 525-529.

[3] W. P. Siriwongpairat, M. Olfat, and K. J. R. Liu, "Performance analysis and comparison of time-hopping and direct-sequence UWB-MIMO systems," *Eurasip Journal on Applied Signal Processing*, vol. 2005, no. 3, pp. 328-345, Mar.2005.

[4] W. P. Siriwongpairat, W. F. Su, M. Olfat, and K. J. R. Liu, "Multiband-OMM MIMO coding framework for UWB communication systems," *ieee Transactions on Signal Processing*, vol. 54, no. 1, pp. 214-224, Jan.2006.

[5] A. Sibille, "Time-domain diversity in ultra-wideband MIMO communications," *Eurasip Journal on Applied Signal Processing*, vol. 2005, no. 3, pp. 316-327, Mar.2005.

[6] C. Prettie, D. Cheung, L. Rusch, and M. Ho, "Spatial Correlation of UWB Signals in a Home Environment," in *IEEE Conference on Ultra Wideband Systems and Technologies* 2004, pp. 65-69.

[7] A. S. Y. Poon and M. Ho, "Indoor Multiple-Antenna Channel Characterization from 2 to 8 GHz," in *Communications, ICC IEEE International Conference on,* 5 ed 2003, pp. 3519-3523.

[8] J. Keignart, C. bou-Rjeily, C. Delaveaud, and N. Daniele, "UWB SIMO channel measurements and simulations," *Ieee Transactions on Microwave Theory and Techniques*, vol. 54, no. 4, pp. 1812-1819, Apr.2006.

[9] I. Z. Kovacs, H. T. Nguyen, P. C. Eggers, and K. Olesen, "Enhanced UWB Radio Channel Model for Short-Range Communication Scenarios Including User Dynamics," in *IST Mobile & Wireless Communications Summit* 2005.

[10] IST 2004-507102, "My Personal Adaptive Global Net (MAGNET) Deliverable 3.1.2a: PAN Radio Channel Characterization (Part 1),"Oct.2004.

[11] N. D. Skentos, A. G. Kanatas, P. I. Dallas, and P. Constantinou, "MIMO channel characterization for short range fixed wireless propagation environments," *Wireless Personal Communications*, vol. 36, no. 4, pp. 339-361, Mar.2006.

[12] G. J. Foschini and M. J. Gans, "On Limits of Wireless Communications in a Fading Environment when Using Multiple Antennas," *Wireless Personal Communications*, vol. 6, no. 3, pp. 311-335, 1998.

[13] M. Herdin and E. Bonek, "A MIMO correlation matrix based metric for characterizing non-stationarity," in *IST Mobile & Wireless Communications Summit* 2004.

[14] J. P. Kermoal, L. Schumacher, K. I. Pedersen, P. E. Mogensen, and F. Frederiksen, "A Stochastic MIMO radio channel model with experimental validation," *ieee Journal on Selected Areas in Communications*, vol. 20, no. 6, pp. 1211-1226, Aug.2002.

[15] K. Yu and B. Ottersten, "Models for MIMO propagation channels: a review," *Wireless Communications & Mobile Computing*, vol. 2, no. 7, pp. 653-666, Nov.2002.

[16] W. Weichselberger, M. Herdin, H. Ozcelik, and E. Bonek, "A stochastic MIMO channel model with joint correlation of both link ends," *ieee Transactions on Wireless Communications*, vol. 5, no. 1, pp. 90-100, Jan.2006.